Electronic Supplementary Material (ESI) for Journal of Materials Chemistry A.
This journal is © The Royal Society of Chemistry 2019

Electronic Supplementary Information

Alloying in inverse CeO_2/Pd nanoparticles to enhance the electrocatalytic activity of formate oxidation reaction

Quan Tang [a,b], Fuyi Chen [*,a,b], Tao Jin [a,b], Longfei Guo [a,b], Qiao Wang [a,b] and Huazhen Liu [a,b]

a. State Key Laboratory of Solidification Processing, Northwestern Polytechnical University, Xian, 710072, China.

b. School of Materials Science and Engineering, Northwestern Polytechnical University, Xi'an, 710072, China.

*Corresponding author. fuyichen@nwpu.edu.cn (Fuyi Chen)

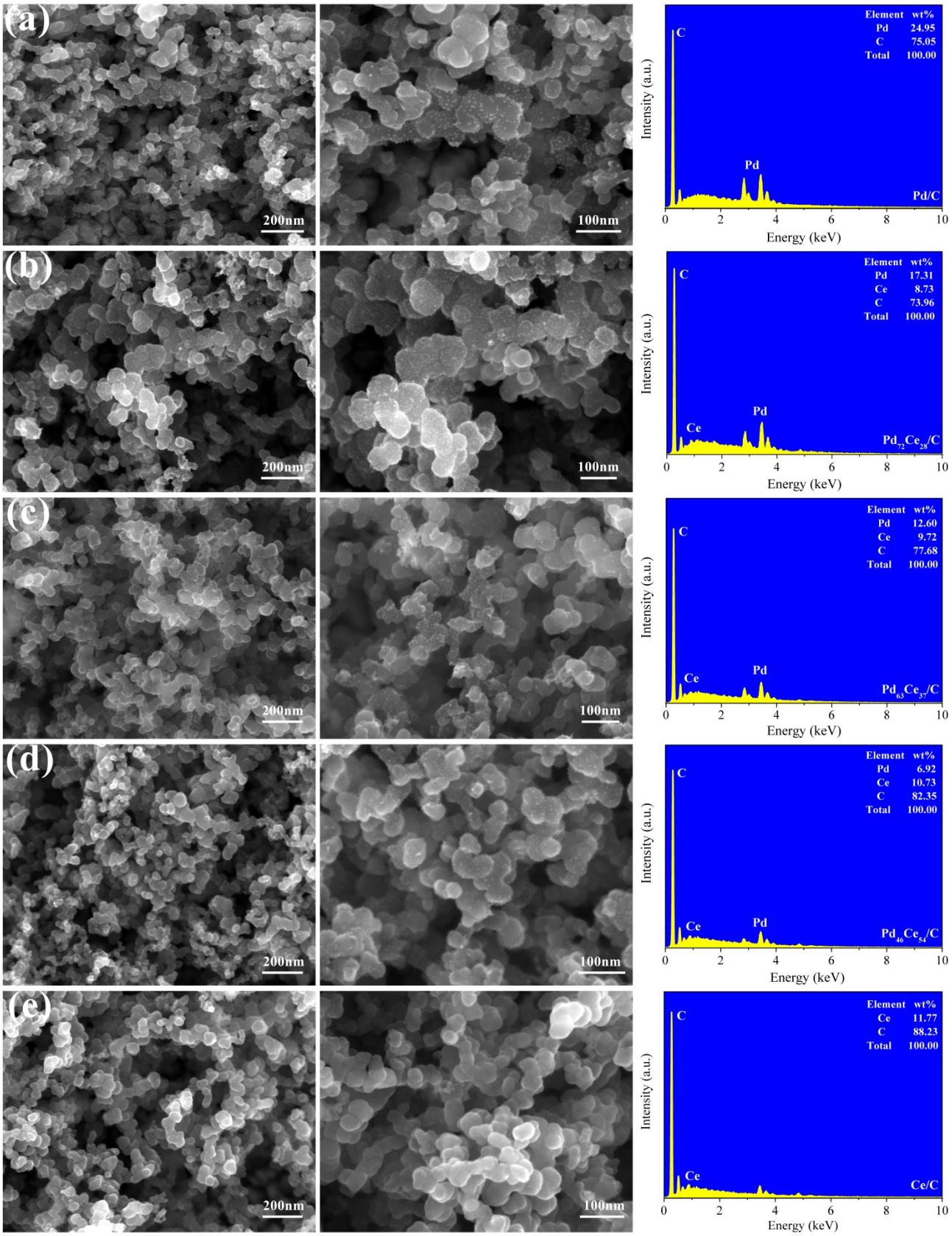

Figure S1. SEM images with different magnifications and the corresponding EDS of the various PdCe/C catalysts. (a) Pd/C, (b) $Pd_{72}Ce_{28}/C$, (c) $Pd_{63}Ce_{37}/C$, (d) $Pd_{46}Ce_{54}/C$ and (e) Ce/C.

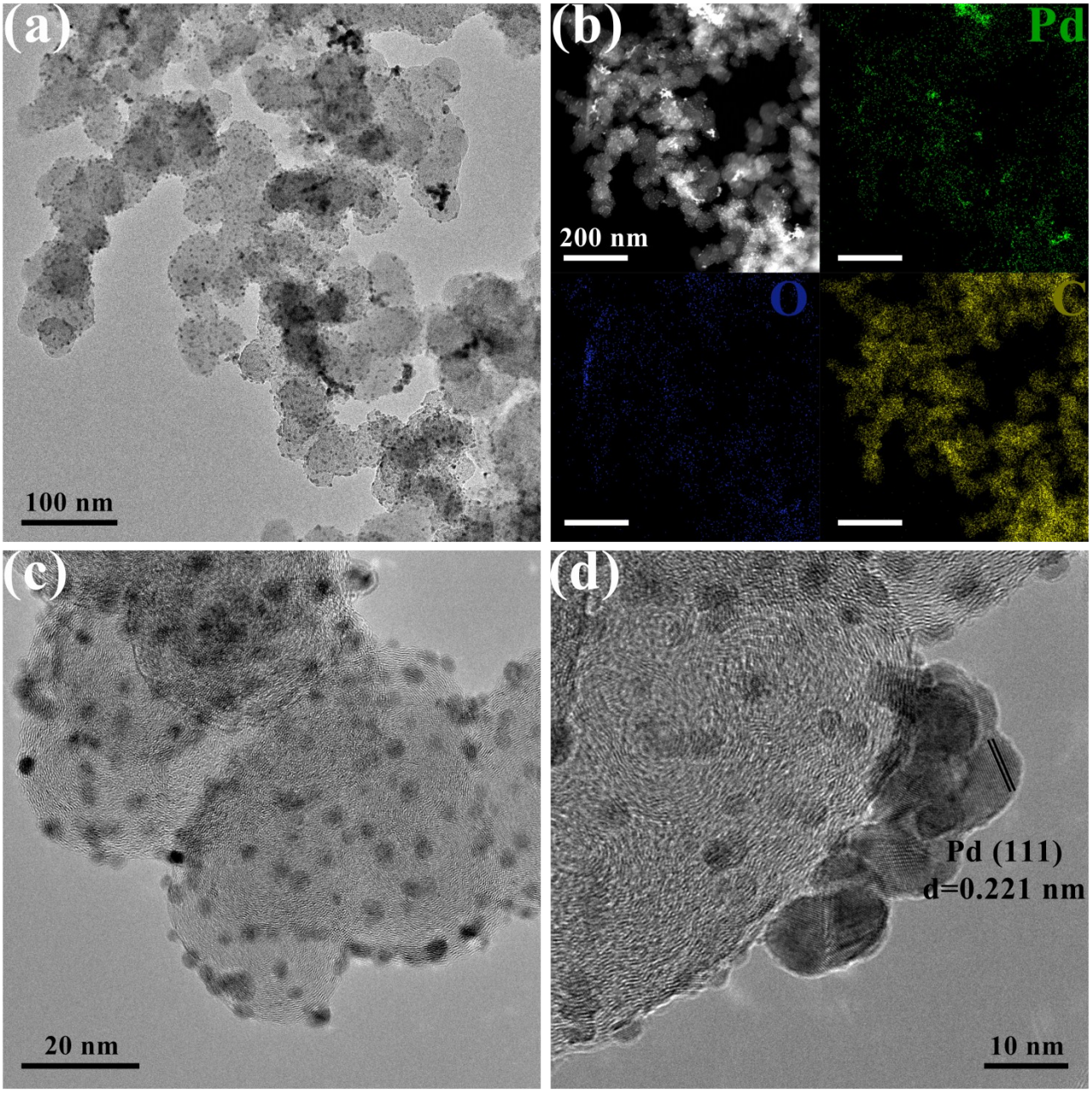

Figure S2. TEM images with different magnifications and the corresponding EDX of Pd/C catalyst. (a) TEM image of Pd/C catalyst. (b) HAADF image and EDX elemental mapping of Pd/C catalyst. (c) TEM image of the carbon supported Pd nanoparticles. (d) The high-resolution TEM image of the carbon supported Pd nanoparticles. The interplanar spacing of the carbon supported Pd nanoparticles could be marked in the image.

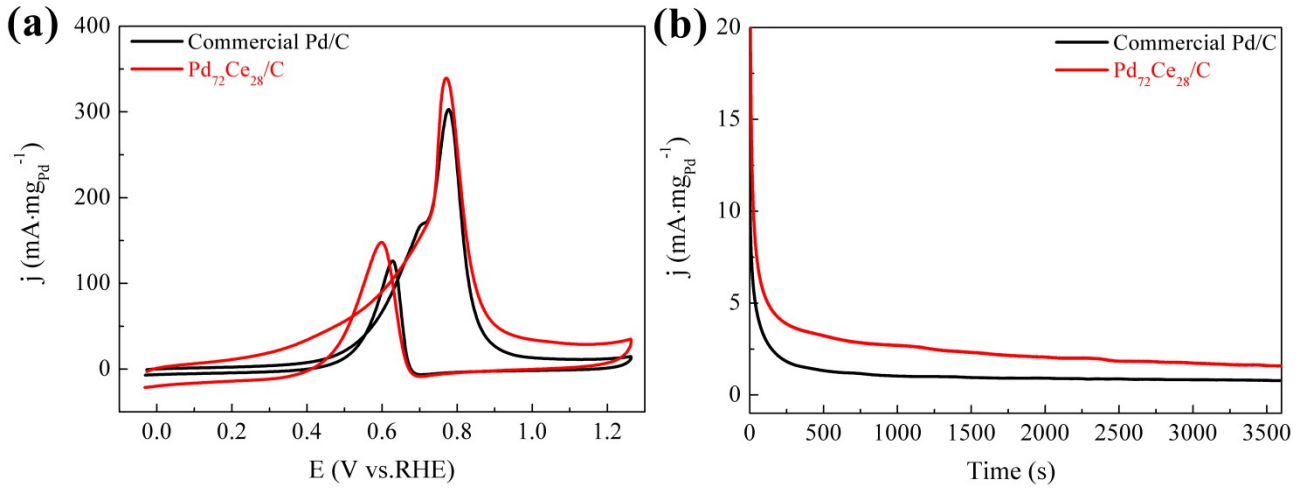

Figure S3. Electrochemical performance of $Pd_{72}Ce_{28}$/C catalysts for the methanol oxidation reaction. (a) CV curves of $Pd_{72}Ce_{28}$/C and the commercial Pd/C catalysts at the scan rate of 50 $mV \cdot s^{-1}$ in N_2-saturated 1 M KOH with 1 M CH_3OH solution normalized by the mass of Pd. (b) CA curves at 0.45 V in N_2-saturated 1 M KOH with 1 M CH_3OH solution.

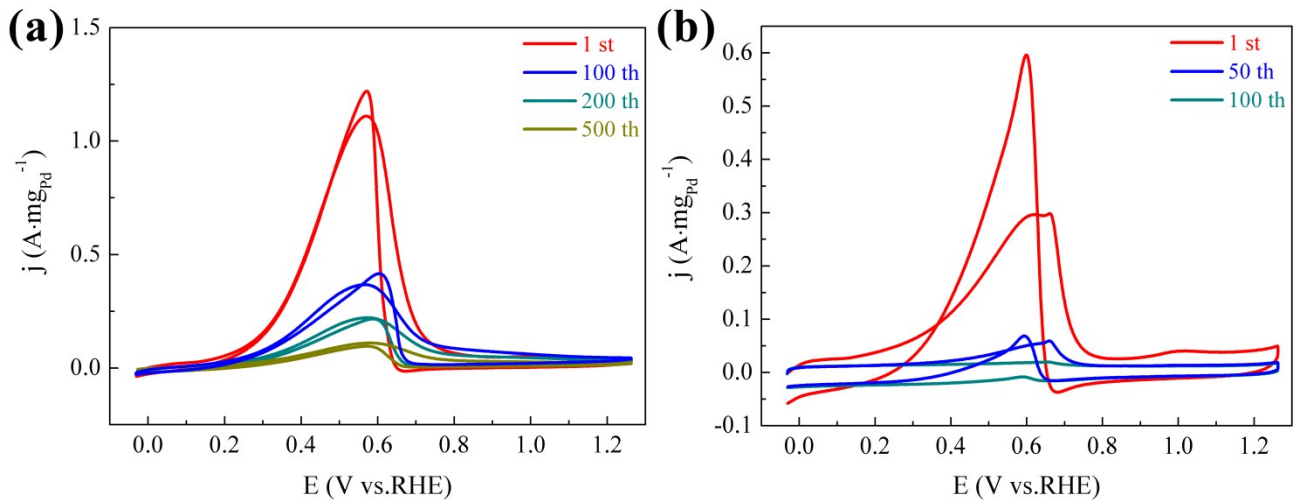

Figure S4. Cycle stability of $Pd_{72}Ce_{28}$/C catalysts for the formate oxidation reaction. CV curves at different cycle times of (a) $Pd_{72}Ce_{28}$/C catalyst and (b) the commercial Pd/C catalyst at the scan rate of 50 $mV \cdot s^{-1}$ in N_2-saturated 1 M KOH with 1 M CH_3OH solution normalized by the mass of Pd.

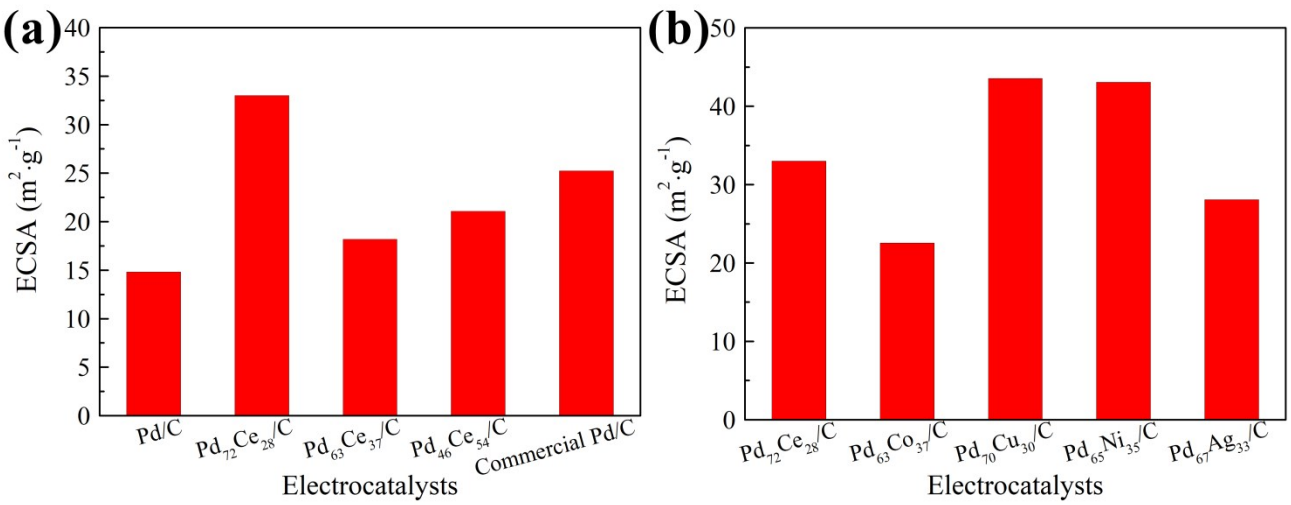

Figure S5. (a) ECSA of $Pd_{72}Ce_{28}/C$ catalyst compared to other PdCe/C catalysts and commercial Pd/C catalyst. (b) ECSA of PdM/C (M = Co, Cu, Ni, Ag) catalysts and $Pd_{72}Ce_{28}/C$ catalyst. All ECSAs are obtained by integrating the reduction peak area of Pd in the CV curves.

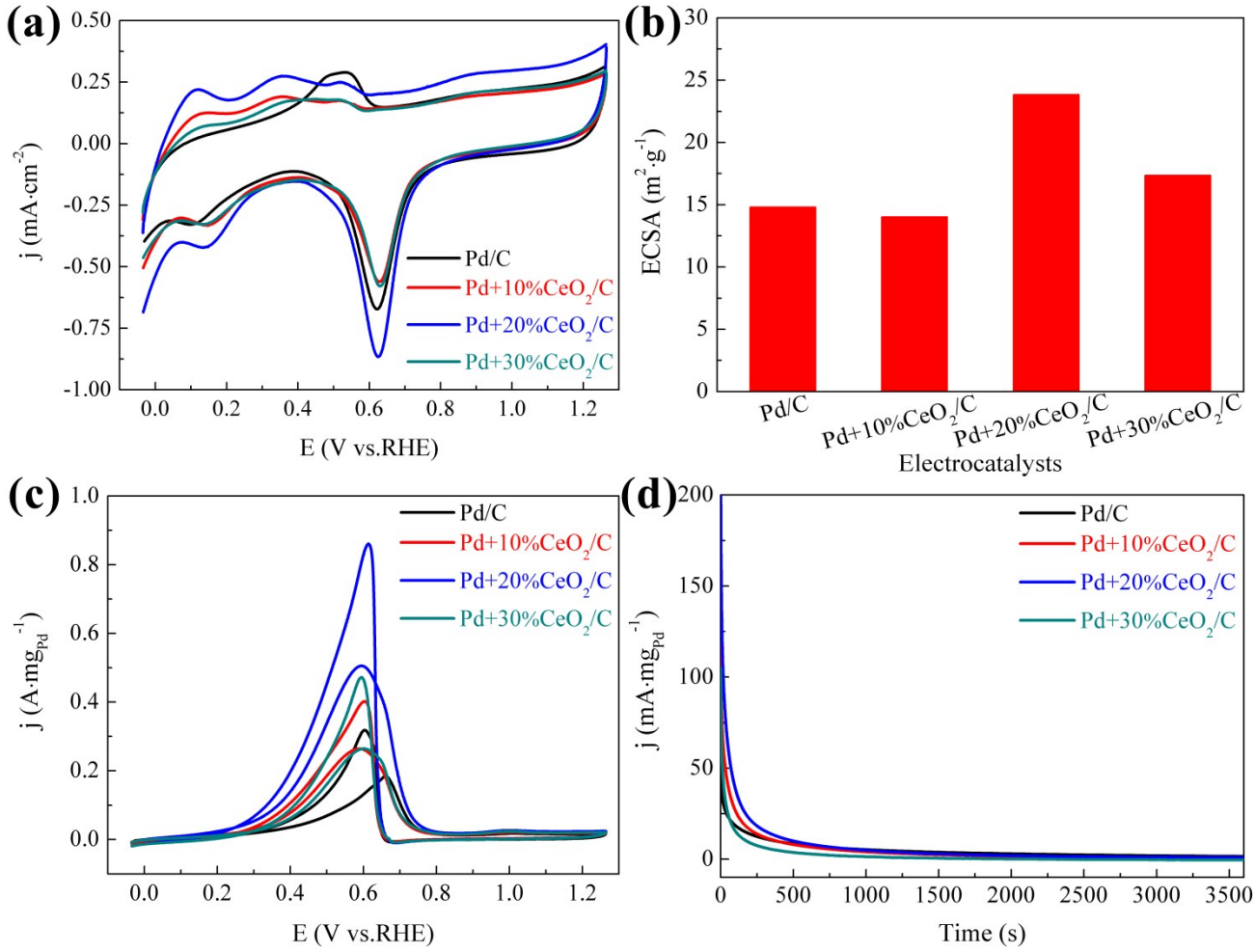

Figure S6. Electrochemical performance of Pd+CeO_2/C mixture catalysts for the formate oxidation reaction. (a) CV curves of Pd/C mix with various percentage CeO_2 catalysts at the scan rate of 50 mV·s^{-1} in N_2-saturated 1 M KOH solution. (b) ECSA of Pd/C mixed with various percentages CeO_2 catalysts. (c) CV curves of Pd/C mixed with various percentages CeO_2 catalysts at the scan rate of 50 mV·s^{-1} in N_2-saturated 1 M KOH with 1 M HCOOK solution normalized by the mass of Pd. (d) CA curves at 0.45 V in N_2-saturated 1M KOH with 1 M HCOOK solution.

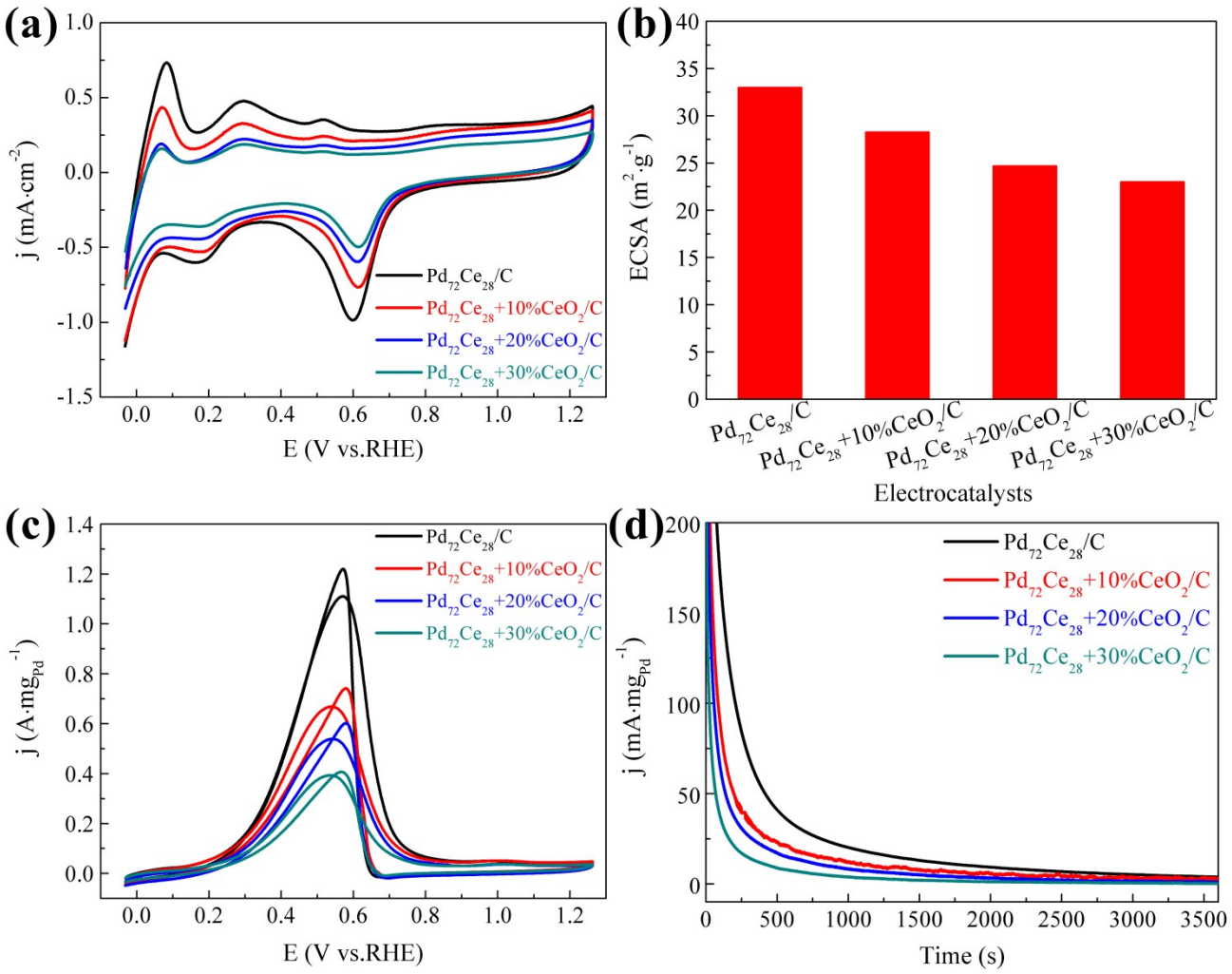

Figure S7. Electrochemical performance of $Pd_{72}Ce_{28}$+CeO_2/C mixture catalysts for the formate oxidation reaction. (a) CV curves of $Pd_{72}Ce_{28}$/C mixed with various percentages CeO_2 catalysts at the scan rate of 50 mV·s^{-1} in N_2-saturated 1 M KOH solution. (b) ECSA of $Pd_{72}Ce_{28}$/C mixed with various percentages CeO_2 catalysts. (c) CV curves of $Pd_{72}Ce_{28}$/C mix with various percentage CeO_2 catalysts at the scan rate of 50 mV·s^{-1} in N_2-saturated 1 M KOH with 1 M HCOOK solution normalized by the mass of Pd. (d) CA curves at 0.45 V in N_2-saturated 1M KOH with 1 M HCOOK solution.

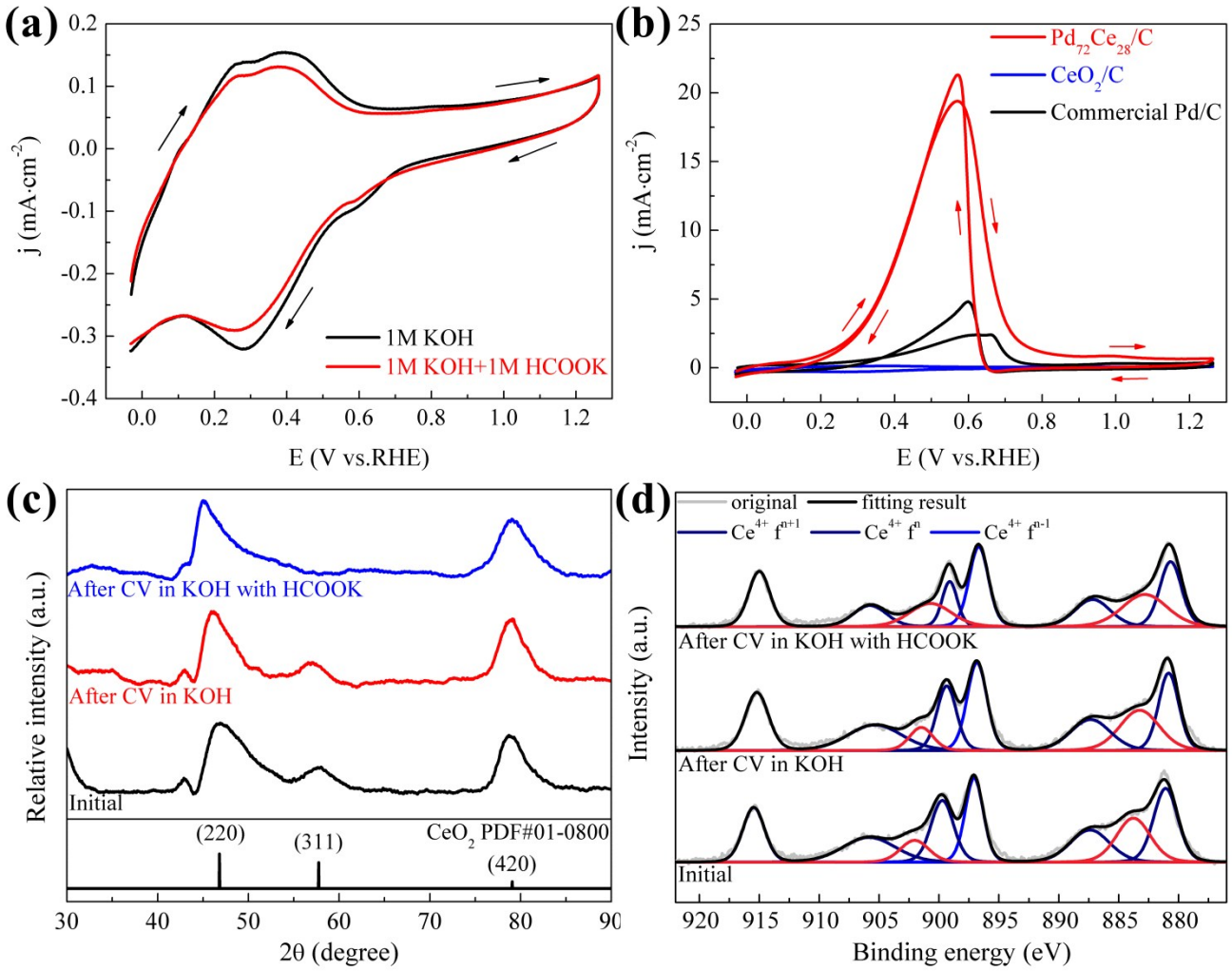

Figure S8. (a) CV curves of CeO_2/C catalyst at the scan rate of 50 mV·s^{-1} in N_2-saturated 1 M KOH solution and 1 M KOH with 1 M HCOOK solution normalised by the geometric area. (b) CV curves of $Pd_{72}Ce_{28}$/C, CeO_2/C and the commercial Pd/C catalysts at the scan rate of 50 mV·s^{-1} in N_2-saturated 1 M KOH with 1 M HCOOK solution normalised by the geometric area. (c) Full-range XRD patterns for the as-prepared CeO_2/C catalyst (black line), the CeO_2/C catalysts after 20 CV cycles in 1 M KOH solution (red line) and the CeO_2/C catalysts after 20 CV cycles 1 M KOH with 1 M HCOOK solution (blue line). The standard XRD patterns for CeO_2 are also provided for reference. (d) High-resolution XPS spectrum of the Ce 3d region for the as-prepared CeO_2/C catalyst, the CeO_2/C catalysts after 20 CV cycles in 1 M KOH solution and the CeO_2/C catalysts after 20 CV cycles in 1 M KOH with 1 M HCOOK solution.

Table S1. Molar ratios of metal precursors during the synthetic process and the EDS composition for different PdCe/C catalysts and the pure monometallic counterparts.

Catalyst name	$Pd(NO_3)_2 \cdot 2H_2O$ (mM)	$Ce(NO_4)_3 \cdot 6H_2O$ (mM)	EDS composition (wt. %)			Atomic ratio (%)
			Pd	Ce	C	Pd/Ce
Pd/C	13.3	0	25.0	0	75.0	100/0
$Pd_{72}Ce_{28}/C$	10.0	3.3	17.3	8.7	74.0	72/28
$Pd_{63}Ce_{37}/C$	6.6	6.6	12.6	9.7	77.7	63/37
$Pd_{46}Ce_{54}/C$	3.3	10.0	6.9	10.7	82.4	46/54
Ce/C	0	13.3	0	11.8	88.2	0/100

Table S2. The XPS surface composition of element Pd in $Pd_{72}Ce_{28}/C$ catalyst and the pure Pd/C counterpart.

Catalyst name		Pd			Pd^{2+}		
		$3d_{5/2}$	$3d_{3/2}$	Total	$3d_{5/2}$	$3d_{3/2}$	Total
Pd/C	BE (eV)	335.7	340.9		336.5	342.3	
	Content (at %)	46.1	32.8	78.9	13.0	8.1	21.1
$Pd_{72}Ce_{28}/C$	BE (eV)	335.9	341.2		337.8	343.2	
	Content (at %)	52.0	35.4	87.4	5.3	7.3	12.6

BE: XPS binding energy.

Table S3. A literature survey of the activity of Pd-based and Pt-based FOR catalysts in alkaline media.

Catalyst	Electrolyte	Scan rate ($mV \cdot s^{-1}$)	Specific activity ($mA \cdot cm^{-2}$)	Mass activity ($A \cdot mg_{Pd}^{-1}$)	Reference
$Pd_{72}Ce_{28}$/C	**1.0 M KOH + 1.0 M HCOOK**	**50**	**19.4**	**1.1**	**This work**
PdH/C	1.0 M KOH + 0.1 M HCOOK	20	0.1	NA	[1]
Pd_4Ag/C	1.0 M NaOH + 0.1 M HCOONa	50	NA	0.04	[2]
PdCu/C	1.0 M KOH + 1.0 M HCOOK	30	3.5	NA	[3]
PdAu/Ni foam	0.5 M NaOH + 0.1 M HCOONa	50	0.8	NA	[4]
CuPdAu/C	0.5 M KOH + 0.5 M HCOOK	50	NA	1.2	[5]
PdAgCu aergels	1.0 M KOH + 1.0 M HCOOK	50	10.1	2.7	[6]
PdAgPt aerogels	0.5 M KOH+ 0.5 M HCOOK	50	3.5	2.9	[7]
$Pd_{2.3}Co$/C	1.0 M KOH + 1.0 M HCOOK	50	NA	2.5	[8]
PdNi/C	1.0 M KOH + 1.0 M HCOOK	50	12.0	4.5	[9]
PdRh/C	1 M KOH + 1.0 M HCOOK	50	8.1	4.5	[10]
Pt-Ag	1 M KOH+ 1.0 M HCOOK	50	NA	0.8	[11]

Table S4. The alloy formation energy, d-band center and Mulliken charge distribution for all slab models, including Pd (111), Pd_3Ce_1 (111), Pd_1Ce_1 (111), Pd_1Ce_3 (111), and Ce (111) surface.

Alloys	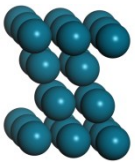 Pd	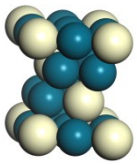 Pd_3Ce_1	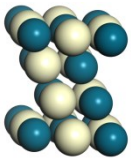 Pd_1Ce_1	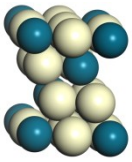 Pd_1Ce_3	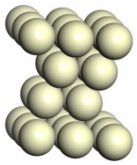 Ce
Total Energy (eV)	-71137.39018	-60682.20106	-50209.89984	-39744.31303	-29274.87698
Formation Energy (eV)		-10.44	-3.77	-3.81	
d-band center (eV)	-2.02	-2.78	-2.59	-1.42	-0.75
Mulliken charge analysis	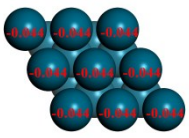	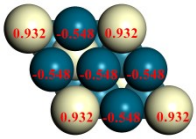	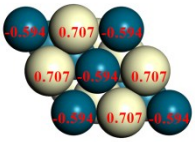	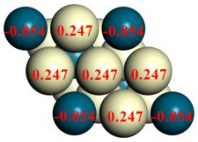	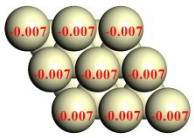

Table S5. The binding energy for H, CO_2 and HCOO on Pd_3Ce_1 (111) surface compare to Pd (111) surface.

Alloys	H	CO_2	HCOO
Pd (111)	-2.47 eV	-0.57 eV	-2.6 eV
Pd_3Ce_1 (111)	-1.04 eV	-0.22 eV	-1.99 eV

Table S6. Hydrogen binding energy (HBE), potential limiting barrier and catalytic activity on the Pd_3Ce_1 (111) and Pd (111) surfaces.

Surface	HBE	ΔG_3	Catalytic activity
Pd (111)	-2.47 eV	0.74 eV	0.29 A·mg_{Pd}^{-1}
Pd_3Ce_1 (111)	-1.04 eV	0.23 eV	1.12 A·mg_{Pd}^{-1}

ΔG_3 denotes the change of free energy for the reaction step (3).

References

1. M. Choun, K. Ham, D. Shin, J. K. Lee and J. Lee, *Catalysis Today*, 2017, **295**, 26-31.
2. S. Roy Chowdhury, S. Ghosh and S. K. Bhattachrya, *Electrochimica Acta*, 2017, **225**, 310-321.
3. J. Noborikawa, J. Lau, J. Ta, S. Hu, L. Scudiero, S. Derakhshan, S. Ha and J. L. Haan, *Electrochimica Acta*, 2014, **137**, 654-660.
4. Y. Li, Y. He and W. Yang, *Journal of Power Sources*, 2015, **278**, 569-573.
5. H. Mao, T. Huang and A. Yu, *International Journal of Hydrogen Energy*, 2016, **41**, 13190-13196.
6. Q. Wang, F. Chen, L. Guo, T. Jin, H. Liu, X. Wang, X. Gong and Y. Liu, *J. Mater. Chem. A*, 2019, DOI: 10.1039/C9TA00664H.
7. J. Wang, F. Chen, Y. Jin, L. Guo, X. Gong, X. Wang and R. L. Johnston, *Nanoscale*, 2019, DOI: 10.1039/C9NR03266E.
8. S. Sankar, G. M. Anilkumar, T. Tamaki and T. Yamaguchi, *ACS Applied Energy Materials*, 2018, **1**, 4140-4149.
9. S. Sasidharan, G. M. Anilkumar, T. Tamaki and T. Yamaguchi, *ChemCatChem*, DOI: 10.1002/cctc.201900960.
10. J. Bai, Q. Xue, Y. Zhao, J.-X. Jiang, J.-H. Zeng, S.-B. Yin and Y. Chen, *ACS Sustainable Chemistry & Engineering*, 2019, **7**, 2830-2836.
11. S.-H. Han, H.-M. Liu, J. Bai, X. L. Tian, B. Y. Xia, J.-H. Zeng, J.-X. Jiang and Y. Chen, *ACS Applied Energy Materials*, 2018, **1**, 1252-1258.